

Stochastic Security-constrained Unit Commitment Considering Electric Vehicles, Energy Storage Systems, and Flexible Loads with Renewable Energy Resources

Ali Gholami Trojani, Mahmoud Samiei Moghaddam, and Javad Mohamadi Baigi

Abstract—In this paper, a new formulation for modeling the problem of stochastic security-constrained unit commitment along with optimal charging and discharging of large-scale electric vehicles, energy storage systems, and flexible loads with renewable energy resources is presented. The uncertainty of renewable energy resources is considered as a scenario-based model. In this paper, a multi-objective function which considers the reduction of operation cost, no-load and startup/shutdown costs, unserved load cost, load shifting, carbon emission, optimal charging and discharging of energy storage systems, and power curtailment of renewable energy resources is considered. The proposed formulation is a mixed-integer linear programming (MILP) model, of which the optimal global solution is guaranteed by commercial solvers. To validate the proposed formulation, several cases and networks are considered for analysis, and the results demonstrate the efficiency.

Index Terms—Electric vehicle, energy storage system, flexible load, renewable energy resource, unit commitment.

I. INTRODUCTION

THE problem of unit commitment is a fundamental optimization task in the management of power systems to determine the optimal set of on/off status of existing units, which minimizes the total operation cost and at the same time meets certain limitations in the short term. The main challenges faced by the problem of unit commitment can be summarized as follows.

One challenge is created by the high penetration of renewable energy resources for power system operators in the unit commitment. Another challenge is the use of grid-connected electric vehicles (EVs) as movable energy storage units with intelligent charging and discharging schedules.

Two basic approaches are to use demand-side management programs and large-scale energy storage systems to increase grid flexibility in the presence of renewable energy resources and grid-connected EVs.

Given the above, the main objectives for power system operators are to provide a mathematical model for unit commitment with security constraints and model the uncertainty of renewable energy resources by modeling EVs and energy storage systems under flexible loads that can lead to finding optimal global solutions.

Reference [1] proposed a formulation of the problem of unit commitment with security constraints considering an iterative solution process without renewable energy resources. Reference [2] proposed a network-constrained clustered unit commitment approach with stochastic medium-term risk-averse programming for the thermal-hydro-wind system without considering the energy storage systems. Reference [3] proposed a meta-heuristic algorithm to solve the non-linear unit commitment problem. In [4], a solution to the unit commitment problem with security constraints was presented considering a hybrid voltage source converter based on multi-terminal power systems with high penetration of wind generation without considering storage batteries. In [5], a branch-and-cut method was proposed to solve the problem of unit commitment without considering the grid security constraints. In [6], a closed-loop forecasting and optimization framework was proposed for the economic improvement of network-constrained unit commitment without the uncertainty of renewable energy resources. In [7], a second-order conic model was proposed to solve the problem of network security-constrained unit commitment based on the Benders decomposition method without considering a multi-objective function, energy storage resources, and renewable energy resources. In [8], a formula for unit commitment with preventive security constraints was proposed by modeling transmission system losses and many fossil resources without considering their emissions and environmental pollution effects. In [9], a general real-data-based framework for the unit commitment with high penetration of renewable energy resources by deep neural networks was proposed to predict the frequency response without considering demand-side manage-

Manuscript received: November 28, 2022; revised: January 3, 2023; accepted: February 22, 2023. Date of CrossCheck: February 22, 2023. Date of online publication: April 21, 2023.

This article is distributed under the terms of the Creative Commons Attribution 4.0 International License (<http://creativecommons.org/licenses/by/4.0/>).

A. G. Trojani and J. M. Baigi are with the Electrical Engineering Department, Damghan Branch, Islamic Azad University, Damghan, Iran (e-mail: ali.trojani@gmail.com; mohamadi.s.j@gmail.com).

M. S. Moghaddam (corresponding author) was with Electrical Engineering Department, Damghan Branch, Islamic Azad University, Damghan, Iran (e-mail: samiei352@yahoo.com).

DOI: 10.35833/MPCE.2022.000781



ment. In [10], a model was proposed for a stochastic security-constrained unit commitment with an energy storage system by mixed-integer programming formulation to reduce operation costs. Reference [11] proposed an approach to solving the problem of stochastic unit commitment by predicting the high penetration of solar resources without considering the outage of lines and power plants. In [12], a simple unit commitment with the EV system connected to the smart grid was proposed without considering the effects of renewable energy resources, uncertainty, and energy storage systems in the grid. In [13], a hierarchical modeling strategy based on the mixed-integer linear programming (MILP) model was proposed to solve the short-term optimal timing problem of hydro units by dividing it into two subsections, i.e., load distribution and unit commitment. Reference [14] proposed a mechanism to optimize the unit commitment based on the production of wind energy scenarios to reduce operation costs without considering energy storage system and smart load management. In [15], a fuzzy MILP model was proposed with a focus on price uncertainty for the issue of monthly single bus unit commitment in a real power grid.

In [16], an MILP model was proposed for the price-based demand response program based on system reliability in the problem of unit commitment with security constraints along with wind farms in the presence of unforeseen events with-

out energy storage systems and power plant emissions. In [17], an MILP model was proposed for the problem of unit commitment with large-scale wind farms considering the demand response problem with multi-time scale flexibility constraints. In [18], a mixed-integer second-order conic model was proposed to solve the unit commitment by modeling different types of power plants. In [19], a non-linear programming model for the multi-area security-constrained unit commitment without storage and flexible demand was proposed. In [20], a robust model was proposed to solve the unit commitment problem with integrated energy storage systems, renewable energy resources, and flexible alternating current transmission system (FACTS) devices to maximize security and minimize costs regardless of demand response.

Table I presents a summary of the aforementioned models for the problem of unit commitment in recently published papers, where ADMM stands for alternating directions method of multipliers; MISOCP stands for mixed-integer second-order cone programming; DICOPT stands for discrete and continuous optimizer; GBO stands for gradient-based optimizer; and MINLP stands for mixed-integer non-linear programming. According to Table I, the proposed formulation of this paper is a complete optimization model compared to other similar papers.

TABLE I
SUMMARY OF PROPOSED FORMULATION AND EXISTING MODELS FOR UNIT COMMITMENT

Reference	Solver	Model	EV	Security	Renewable	Multi-objective	Stochastic	Flexible load	Battery	Emission
This paper	Gurobi	MILP	✓	✓	✓	✓	✓	✓	✓	✓
[1]	Gurobi	MILP		✓						
[2]	Cplex	MISOCP		✓	✓		✓			
[3]	GBO	MINLP								
[4]	Cplex	MILP		✓	✓		✓			
[5]	Gurobi	MILP								
[6]	Cplex	MILP		✓	✓	✓				
[7]	Cplex	MIP		✓	✓					
[8]	Xpress	MILP		✓		✓				
[9]	Gurobi	MILP		✓	✓	✓				
[10]	Cplex	MILP		✓	✓		✓		✓	
[11]	Gurobi	MILP			✓		✓		✓	
[12]	Cplex	MILP	✓							
[13]	Gurobi	MILP			✓	✓				
[14]	Gurobi	MILP			✓		✓			
[15]	Cplex	MILP					✓			
[16]	DICOPT	MILP		✓	✓	✓	✓	✓		
[17]	Gurobi	MILP			✓			✓		
[18]	Gurobi	MISOCP			✓					
[19]	ADMM	MINLP		✓		✓				
[20]	Cplex	MILP		✓	✓	✓			✓	

According to the aforementioned literature review and the comparison of previous models, it can be found that in most of the previous studies, there was no single or complete model considering the modeling of the demand-side management problem, multi-objective functions, stochastic model,

EVs, security constraints, and renewable energy resources in the problem of unit commitment. Thus, in this study, we try to present a complete model considering all these issues.

The main innovations and contributions of this paper can be summarized as follows.

1) A new formulation is introduced for the problem of unit commitment considering the optimal charging and discharging of large-scale EVs, energy storage systems, and flexible loads with renewable energy resources.

2) The uncertainty of renewable energy resources is considered as a scenario-based model.

3) A framework in the form of MILP model with an optimal global solution guaranteed is proposed.

4) A multi-objective function is considered in the proposed formulation, which includes the reduction of operation cost, no-load and startup/shutdown costs, unserved load cost, load shifting, carbon emission, optimal charging and discharging of energy storage systems, and power curtailment of renewable energy resources.

The remainder of this paper is organized as follows. The proposed formulation is presented and fully explained in Section II. The results obtained from the simulation are analyzed in Section III. Finally, the conclusions and some suggestions are presented in Section IV.

II. PROPOSED FORMULATION

The modeling of the problem for stochastic security-constrained unit commitment is presented in this section. Equation (1) demonstrates the objective function of the problem, which considers the reduction of operation cost, no-load and startup/shutdown costs, unserved load cost, load shifting, carbon emission, optimal charging and discharging of energy storage systems, and power curtailment of renewable energy resources. The uncertainty of renewable energy resources is considered as a scenario-based model.

$$\begin{aligned} \min \sum_{b=1}^B \sum_{t=1}^T [& g_{b,t} c_b^g + s_{b,t} c_b^{nl} + u_{b,t} c_b^{su} + d_{b,t} c_b^{sd} + r_{b,t} c_b^{cr} + \\ & (pc_{b,t}^{ess} + pd_{b,t}^{ess}) c_b^{ess} + (d_{b,t}^{in} + d_{b,t}^{dsm}) c_b^{dsm} + g_{b,t} c_b^{emi}] + \\ & \sum_{s=1}^S \pi_s \sum_{b=1}^B \sum_{t=1}^T (g_{b,t,s}^r - g_{b,t}^r) c_b^r \end{aligned} \quad (1)$$

where B , T , and S are the sets of bus, time, and scenario, respectively; b , t , and s are the indices of bus, time, and scenario, respectively; $g_{b,t}$ is the power of the units on bus b at time t ; c_b^g is the unit production cost on bus b ; $s_{b,t}$ is the state of commitment of units on bus b at time t ; c_b^{nl} is the no-load cost of each unit on bus b ; $u_{b,t}$ and $d_{b,t}$ are the on and off statuses of the units on bus b at time t , respectively, and their related costs are c_b^{su} and c_b^{sd} ; $r_{b,t}$ is the load curtailment on bus b at time t ; c_b^{cr} is the cost related to the load interruption; $pc_{b,t}^{ess}$ and $pd_{b,t}^{ess}$ are the charging and discharging power of the battery on bus b at time t , respectively; c_b^{ess} is the cost of charging and discharging of the battery on bus b ; $d_{b,t}^{in}$ is the initial load on bus b at time t ; $d_{b,t}^{dsm}$ is the shifted load after the demand-side management program; c_b^{dsm} is the cost associated with the change or load shedding on bus b in the demand-side management program; c_b^{emi} is the emission cost of the units in bus b ; π_s is the probability of each scenario; $g_{b,t,s}^r$ is the actual production of renewable energy resources on bus b at time t in scenario s ; $g_{b,t}^r$ is the operation power from renewable energy resources on bus b at time t ; and c_b^r is the cost of a power outage of renewable energy resources

on bus b .

The problem of security-constrained unit commitment is also shown by (2)-(14). Equation (2) shows the constraint of power balance on each network bus at time t . Formula (3) shows the limitation of operation of the units. Formula (4) shows the limitation of power flow in each grid line. Formula (5) is the definition of the power flow in each grid line. The load curtailment limit on each bus at time t is indicated by (6). Formula (7) shows the voltage angle limit of each bus at time t . Formula (8) shows the angle limitation of the reference bus voltage. The operating limit of each renewable unit of bus b at time t in scenario s is shown with (9). Formula (10) shows the relationship between binary variables in the problem of unit commitment. Formula (11) shows the line outage in the network. Formula (12) indicates the up and down power ramp limits of the units. Formulas (13) and (14) indicate the minimum up and down time of the units, respectively.

$$g_{b,t} + r_{b,t} + pd_{b,t}^{ess} + g_{b,t}^r + \sum_{ij \in B} f_{ij,t} - \sum_{ji \in B} f_{ji,t} + p_{b,t}^{ev} = pc_{b,t}^{ess} + d_{b,t}^{dsm} \quad \forall b \in B, \forall t \in T \quad (2)$$

$$g_b^{\min} s_{b,t} \leq g_{b,t} \leq g_b^{\max} s_{b,t} \quad \forall b \in B, \forall t \in T, s_{b,t} \in \{0,1\} \quad (3)$$

$$-f_l^{\max} x_l \leq f_{l,t} \leq f_l^{\max} x_l \quad \forall l \in L, \forall t \in T, x_l \in \{0,1\} \quad (4)$$

$$f_{l,t} = x_l B_l (\theta_{i,t} - \theta_{j,t}) \quad \forall l \in L, \forall t \in T, ij \in L \quad (5)$$

$$0 \leq r_{b,t} \leq d_{b,t}^{dsm} \quad \forall b \in B, \forall t \in T \quad (6)$$

$$-\pi \leq \theta_{b,t} \leq \pi \quad \forall b \in B, \forall t \in T \quad (7)$$

$$\theta_{b,t} = 0 \quad \forall b = r_{ef}, \forall t \in T \quad (8)$$

$$0 \leq g_{b,t}^r \leq g_{b,t,s}^r \quad \forall b \in B, \forall t \in T, \forall s \in S \quad (9)$$

$$s_{b,t} - s_{b,t-1} = u_{b,t} - d_{b,t} \quad \forall b \in B, \forall t \in T \quad (10)$$

$$\sum_{l=1}^L x_l = L - k \quad (11)$$

$$-r_b^{dw} \leq g_{b,t+1} - g_{b,t} \leq r_b^{up} \quad \forall b \in B, \forall t \in T \quad (12)$$

$$\sum_{k=t-UT_b+1}^t u_{b,k} \leq s_{b,t} \quad \forall b \in B, t \in \{UT_b, \dots, T\} \quad (13)$$

$$\sum_{k=t-DT_b+1}^t d_{b,k} \leq 1 - s_{b,t} \quad \forall b \in B, t \in \{DT_b, \dots, T\} \quad (14)$$

where $f_{ij,t}$ is the power flow from bus i to j ; $f_{ji,t}$ is the power flow from bus j to i ; $p_{b,t}^{ev}$ is the injected or received power of the EVs on bus b at time t ; g_b^{\min} and g_b^{\max} are the lower and upper limits of the power of the units on bus b , respectively; L is the set of grid lines; l is the index of line; x_l is the state of lines, if it is equal to 1, the line is connected, and if it is equal to 0, the line is disconnected; f_l^{\max} is the maximum power flow through line l ; B_l is the susceptance of line l ; $\theta_{i,t}$ is the voltage angle of bus i at time t ; k is the number of lines disconnected from the network; r_{ef} is the set of reference buses; $f_{l,t}$ is the real power flow; r_b^{dw} and r_b^{up} are the minimum and maximum ramp rates, respectively; UT_b is the minimum up time; and DT_b is the minimum down time.

Relationships (15)-(26) show the modeling of EVs in the problem of security-constrained unit commitment. The net charging and discharging energy of the EV battery is shown in (15) according to the efficiency of each battery. Equation (16) shows the amount of power injected and received from or to the network by EVs, which is calculated by the charging and discharging rate of the battery. The charging and discharging statuses of EVs are shown in (17). Formulas (18) and (19) show the limitations of charging and discharging power of EVs, respectively. Formula (20) shows the energy status of the EV battery. Formula (21) shows the limitation of battery energy capacity in EVs. Formulas (22) and (23) consider the net charging and discharging energy and the available energy of the EV battery in the first and last hours. Formulas (24)-(26) show the charging and discharging costs of EV batteries.

$$e_{b,t}^{net,ev} = p_{b,t}^{dis,ev} - \eta_b^{ev} p_{b,t}^{ch,ev} \quad \forall b \in B, \forall t \in T \quad (15)$$

$$p_{b,t}^{ev} = p_{b,t}^{dis,ev} - p_{b,t}^{ch,ev} \quad \forall b \in B, \forall t \in T \quad (16)$$

$$I_{b,t}^{dis,ev} + I_{b,t}^{ch,ev} = n_{b,t}^{ev} \quad \forall b \in B, \forall t \in T \quad (17)$$

$$I_{b,t}^{ch,ev} \underline{p}_b^{ch,ev} \leq p_{b,t}^{ch,ev} \leq I_{b,t}^{ch,ev} \bar{p}_b^{ch,ev} \quad \forall b \in B, \forall t \in T \quad (18)$$

$$I_{b,t}^{dis,ev} \underline{p}_b^{dis,ev} \leq p_{b,t}^{dis,ev} \leq I_{b,t}^{dis,ev} \bar{p}_b^{dis,ev} \quad \forall b \in B, \forall t \in T \quad (19)$$

$$e_{b,t}^{ev} = e_{b,t-1}^{ev} - e_{b,t}^{net,ev} - (1 - n_{b,t}^{ev}) dr_{b,t}^{ev} \quad \forall b \in B, \forall t \in T \quad (20)$$

$$\underline{e}_{b,t}^{ev} \leq e_{b,t}^{ev} \leq \bar{e}_{b,t}^{ev} \quad \forall b \in B, \forall t \in T \quad (21)$$

$$e_{b,t=1}^{ev} = e_{b,t=24}^{ev} \quad \forall b \in B \quad (22)$$

$$e_{b,t=1}^{net,ev} = e_{b,t=24}^{net,ev} \quad \forall b \in B \quad (23)$$

$$c_{b,t}^{ev} = n_{b,t}^{ev} \sum_{k=1}^K \beta_{k,b}^{ev} p_{k,b,t}^{ev} \quad \forall b \in B, \forall t \in T \quad (24)$$

$$\begin{cases} n_{b,t}^{ev} (e_{b,t}^{ev} - e_{b,t-1}^{ev}) \geq - \sum_{k=1}^K p_{k,b,t}^{ev} \\ n_{b,t}^{ev} (e_{b,t}^{ev} - e_{b,t-1}^{ev}) \leq \sum_{k=1}^K p_{k,b,t}^{ev} \end{cases} \quad \forall b \in B, \forall t \in T \quad (25)$$

$$0 \leq p_{k,b,t}^{ev} \leq \bar{p}_{k,t}^{ev} \quad \forall b \in B, \forall t \in T \quad (26)$$

where $e_{b,t}^{net,ev}$ is the net charging and discharging energy of the EV battery on bus b at time t ; $p_{b,t}^{dis,ev}$ and $p_{b,t}^{ch,ev}$ are the discharging and charging power of EV batteries on bus b at time t , respectively; η_b^{ev} is the charging efficiency of the EV battery; $I_{b,t}^{dis,ev}$ and $I_{b,t}^{ch,ev}$ are the charging and discharging statuses of EVs on bus b at time t , respectively; $n_{b,t}^{ev}$ is the state of connection to the network of EVs, if it is equal to 1, the EV is connected to the grid, otherwise, it is disconnected; $\underline{p}_b^{ch,ev}$ and $\bar{p}_b^{ch,ev}$ are the minimum and maximum charging power of EVs, respectively; $\underline{p}_b^{dis,ev}$ and $\bar{p}_b^{dis,ev}$ are the minimum and maximum discharging power of EVs, respectively; $e_{b,t}^{ev}$ is the energy status of the EV battery; $dr_{b,t}^{ev}$ is the energy demand of EVs on bus b at time t ; $\underline{e}_{b,t}^{ev}$ and $\bar{e}_{b,t}^{ev}$ are the minimum and maximum energies of the EV battery, respectively; $c_{b,t}^{ev}$ is the operation cost of EVs; $\beta_{k,b}^{ev}$ is the slope of the k^{th} piece for linearizing the cost curve; $p_{k,b,t}^{ev}$ is the power of the k^{th} piece of EVs; $\bar{p}_{k,t}^{ev}$ is the maximum power considered for

the k^{th} piece in linearization; and K is the set of pieces of the curve.

Formulas (27)-(32) represent the energy storage system (battery) in problem of unit commitment. Formulas (27) and (28) show the minimum and maximum discharging and charging capacities of the battery, respectively. Formula (29) indicates the energy in the battery. Formula (30) indicates the minimum and maximum energy limits in the battery, respectively. Formulas (31) and (32) show the initial capacity and energy status of the battery at time $t=1$.

$$0 \leq p d_{b,t}^{ess} \leq \bar{e}_b^{ess} z_{b,t}^{ess} \quad \forall b \in B, \forall t \in T \quad (27)$$

$$0 \leq p c_{b,t}^{ess} \leq \bar{e}_b^{ess} (1 - z_{b,t}^{ess}) \quad \forall b \in B, \forall t \in T \quad (28)$$

$$e_{b,t}^{ess} = e_{b,t-1}^{ess} + p c_{b,t}^{ess} \eta_{ess} - p d_{b,t}^{ess} / \eta_{ess} \quad \forall b \in B, \forall t \in T \quad (29)$$

$$0 \leq e_{b,t}^{ess} \leq \bar{e}_b^{ess} \quad \forall b \in B, \forall t \in T \quad (30)$$

$$e_{b,t=1}^{ess} = \alpha_b \quad \forall b \in B \quad (31)$$

$$e_{b,t}^{ess} = p c_{b,t}^{ess} \eta_{ess} - p d_{b,t}^{ess} / \eta_{ess} \quad \forall b \in B, t=1 \quad (32)$$

where $z_{b,t}^{ess}$ is the battery status; \bar{e}_b^{ess} is the maximum battery capacity on bus b ; $e_{b,t}^{ess}$ is the energy in the battery on bus b at time t ; η_{ess} is the battery efficiency; and α_b is the amount of initial energy in the battery on bus b .

Relationships (33)-(35) represent the demand-side management model in the problem of unit commitment. Formula (33) ensures that the shifted loads after the demand-side management program are less than or equal to the initial network loads per bus. Formulas (33) and (34) show the load changes on bus b at time t in the demand-side management program.

$$\sum_{t \in T} d_{b,t}^{dsm} \leq \sum_{t \in T} d_{b,t}^{in} \quad \forall b \in B \quad (33)$$

$$d_{b,t}^{dsm} \geq d_{b,t}^{in} - d_{b,t}^{in} \omega \quad \forall b \in B, \forall t \in T \quad (34)$$

$$d_{b,t}^{dsm} \leq d_{b,t}^{in} + d_{b,t}^{in} \omega \quad \forall b \in B, \forall t \in T \quad (35)$$

where $d_{b,t}^{dsm}$ is the shifted demand; $d_{b,t}^{in}$ is the initial demand; and ω is the percentage of load changes.

III. SIMULATION RESULTS

To analyze the proposed formulation, two test networks (6-bus and 24-bus) are considered for analysis. The simulation is implemented using Julia programming language and solved with the Gurobi solver. A computer system with a 1.8 GHz CPU and 6 GB RAM is used.

A. 6-bus Network

In this subsection, the results related to the 6-bus network are presented [21]. Figure 1 shows a schematic of the 6-bus network. As observed from Fig. 1, the energy storage system (battery) is located on buses 1 and 3 (ESS 1 and ESS 2), renewable energy resources are installed on buses 2 and 5, and the parking of EVs is located on buses 2, 4, and 6. The network load is on buses 1, 4, 5, and 6, and five power plant units are on buses 1, 2, 3, 5, and 6 (U1-U5). The available 9 transmission lines are indicated by the dashed line. The scenarios for renewable energy resources shown in Fig. 2 are generated according to [22]. The scenario generation method

is mentioned in Appendix A. As can be observed in Fig. 2, the amount of power generated by the photovoltaic (PV) is the highest at the 13th hour, and the scenarios considered for this hour are between 0.8 and 1 p.u.. According to Fig. 2, the maximum production of the wind power plant is at the 12th hour.

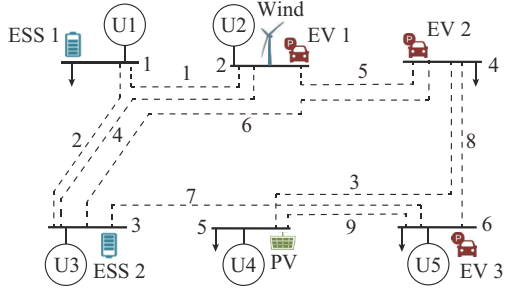


Fig. 1. Schematic of 6-bus network.

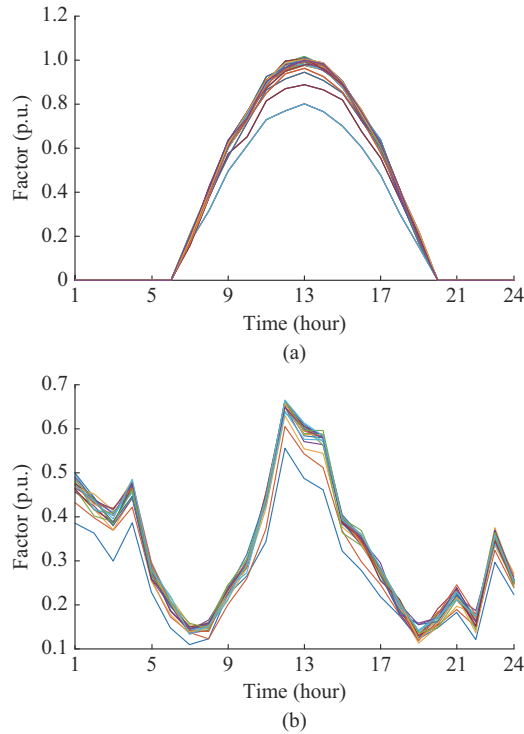


Fig. 2. Generated scenarios for renewable energy resources. (a) Scenarios for PV. (b) Scenarios for wind power.

To better analyze the proposed formulation, four different case studies are considered as follows.

Case 1: considering a maximum of 0% load shifting and the number of outage lines is equal to 1.

Case 2: considering a maximum of 10% load shifting and the number of outage lines is equal to 1.

Case 3: considering a maximum of 0% load shifting and the number of outage lines is equal to 3.

Case 4: considering a maximum of 10% load shifting and the number of outage lines is equal to 3.

The results related to different cases in the 6-bus network are presented in Table II. It can be observed that case 2 has the lowest objective function value.

TABLE II
SIMULATION RESULTS OF DIFFERENT CASES IN 6-BUS NETWORK

Case	Objective function value (\$)	No. of disconnected line
Case 1	535887	9
Case 2	529545	9
Case 3	535890	2, 8, 9
Case 4	529738	4, 8, 9

Figures 3-6 show the status of unit commitment in the 6-bus network in cases 1-4 for the day-ahead operation (1-24 hours). The numbers 1 and 0 indicate that the unit is on and off, respectively. It can be observed that with the change of load shifting and the number of outage lines, the status of unit commitment changes. As can be observed from Figs. 3-6, Unit 3 is on in all cases, which can be due to the low price of this unit. Meanwhile, Unit 1 has different statuses of unit commitment in different cases.

Unit	1	2	3	4	5	6	7	8	9	10	11	12	13	14	15	16	17	18	19	20	21	22	23	24
Unit 1	0	0	0	0	0	0	0	0	0	0	1	1	1	1	1	1	1	1	1	1	1	0	0	0
Unit 2	0	0	0	0	0	0	0	0	0	0	0	0	0	0	0	0	0	0	0	0	0	0	0	0
Unit 3	1	1	1	1	1	1	1	1	1	1	1	1	1	1	1	1	1	1	1	1	1	1	1	1
Unit 4	0	0	0	0	0	0	0	0	0	0	0	0	0	0	0	0	0	0	0	0	0	0	0	0
Unit 5	0	0	0	0	0	0	0	0	0	0	0	0	0	0	0	0	0	0	0	0	0	0	0	0
Unit 6	0	0	0	0	0	0	0	0	0	0	0	0	0	0	0	0	0	0	0	0	0	0	0	0

Fig. 3. Status of unit commitment in 6-bus network in case 1.

Unit	1	2	3	4	5	6	7	8	9	10	11	12	13	14	15	16	17	18	19	20	21	22	23	24
Unit 1	0	0	0	0	0	0	0	0	0	0	1	1	1	1	1	1	1	1	1	1	1	0	0	0
Unit 2	0	0	0	0	0	0	0	0	0	0	0	0	0	0	0	0	0	0	0	0	0	0	0	0
Unit 3	1	1	1	1	1	1	1	1	1	1	1	1	1	1	1	1	1	1	1	1	1	1	1	1
Unit 4	0	0	0	0	0	0	0	0	0	0	0	0	0	0	0	0	0	0	0	0	0	0	0	0
Unit 5	0	0	0	0	0	0	0	0	0	0	0	0	0	0	0	0	0	0	0	0	0	0	0	0
Unit 6	0	0	0	0	0	0	0	0	0	0	0	0	0	0	0	0	0	0	0	0	0	0	0	0

Fig. 4. Status of unit commitment in 6-bus network in case 2.

Unit	1	2	3	4	5	6	7	8	9	10	11	12	13	14	15	16	17	18	19	20	21	22	23	24
Unit 1	0	0	0	0	0	0	0	0	0	0	1	1	1	1	1	1	1	1	1	1	1	0	0	0
Unit 2	0	0	0	0	0	0	0	0	0	0	0	0	0	0	0	0	0	0	0	0	0	0	0	0
Unit 3	1	1	1	1	1	1	1	1	1	1	1	1	1	1	1	1	1	1	1	1	1	1	1	1
Unit 4	0	0	0	0	0	0	0	0	0	0	0	0	0	0	0	0	0	0	0	0	0	0	0	0
Unit 5	0	0	0	0	0	0	0	0	0	0	0	0	0	0	0	0	0	0	0	0	0	0	0	0
Unit 6	0	0	0	0	0	0	0	0	0	0	0	0	0	0	0	0	0	0	0	0	0	0	0	0

Fig. 5. Status of unit commitment in 6-bus network in case 3.

Unit	1	2	3	4	5	6	7	8	9	10	11	12	13	14	15	16	17	18	19	20	21	22	23	24
Unit 1	0	0	0	0	0	0	0	0	0	0	1	1	1	1	1	1	1	1	1	1	1	0	0	0
Unit 2	0	0	0	0	0	0	0	0	0	0	0	0	0	0	0	0	0	0	0	0	0	0	0	0
Unit 3	1	1	1	1	1	1	1	1	1	1	1	1	1	1	1	1	1	1	1	1	1	1	1	1
Unit 4	0	0	0	0	0	0	0	0	0	0	0	0	0	0	0	0	0	0	0	0	0	0	0	0
Unit 5	0	0	0	0	0	0	0	0	0	0	0	0	0	0	0	0	0	0	0	0	0	0	0	0
Unit 6	0	0	0	0	0	0	0	0	0	0	0	0	0	0	0	0	0	0	0	0	0	0	0	0

Fig. 6. Status of unit commitment in 6-bus network in case 4.

Figure 7 illustrates the optimal charging and discharging statuses of EV parking in cases 1-4 over a 24-hour period, where SOC stands for state of charge. The negative vertical

axis indicates the charging status of EV parking, while the positive vertical axis indicates the discharging status. The optimal charging and discharging statuses of EV parking located on buses 2, 4, and 6 are shown in blue, purple, and orange, respectively. It can be observed that in each case, the charging and discharging statuses of EV parking are different. Fig. 7 proves that the proposed formulation for EV parking performs well in each case. Similarly, Fig. 8 shows the state of energy (SOE) of EVs in cases 1-4 in the 6-bus network over a 24-hour period. It can be observed that the SOE level is generally lower at the 5th to 10th hours than that at other hours, which is a sign of power discharging of EVs.

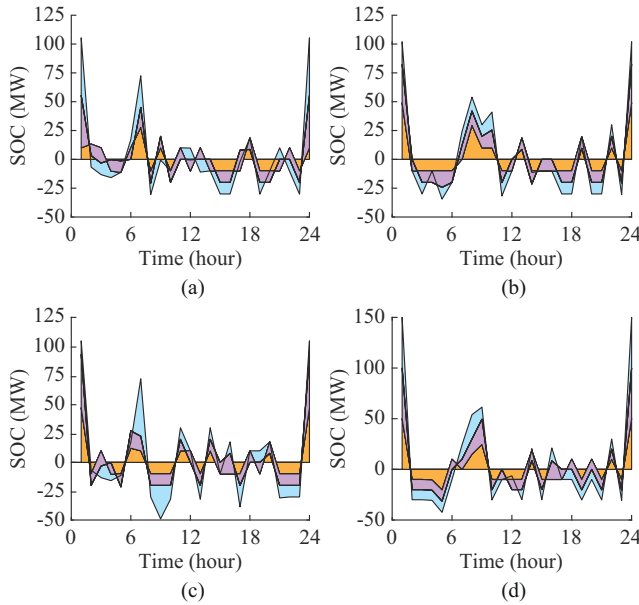


Fig. 7. Comparison of charging and discharging status of EV parking in 6-bus network. (a) Case 1. (b) Case 2. (c) Case 3. (d) Case 4.

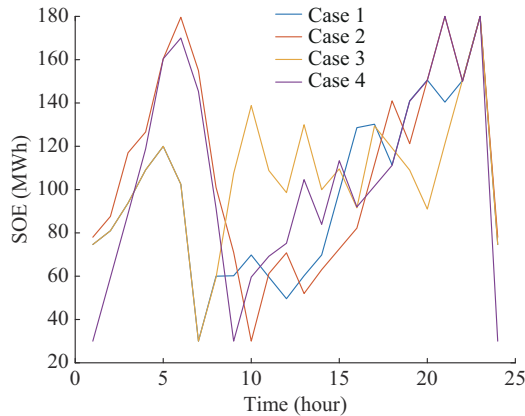


Fig. 8. Comparison of SOE of EVs in cases 1-4 in 6-bus network.

Figure 9 demonstrates the optimal charging and discharging statuses of the energy storage system in cases 1-4, where the blue and yellow columns represent the energy storage system located on buses 1 and 3, respectively. As can be observed, in all cases, the energy storage systems are discharged when the energy purchase price is high and are charged when the energy purchase price is low. It should al-

so be noted that in addition to the energy price, other indicators in the objective function of the problem also affect the optimal charging and discharging of the energy storage system. Similarly, Fig. 10 shows the status of energy remaining in the energy storage system. As can be observed from Figs. 9 and 10, whenever the energy storage system is charged according to Fig. 9, its energy capacity increases in Fig. 10, and whenever the energy storage system is discharged according to Fig. 9, its capacity decreases in Fig. 10. Figure 11 illustrates a comparison of the load shifting in each case in the 6-bus network, which shows the exact performance of the proposed demand-side management model. Since load shifting is not considered in the cases 1 and 3, the case 3 is not shown to avoid repetition. It can be observed that the load shifting is different in different cases. Figure 12 demonstrates the production of units in different cases in the day-ahead operation in the 6-bus network. It can be observed when the network load increases during the 10th to 21st hours, the production of units increases, which is a sign of the accurate performance of the power balance in the network.

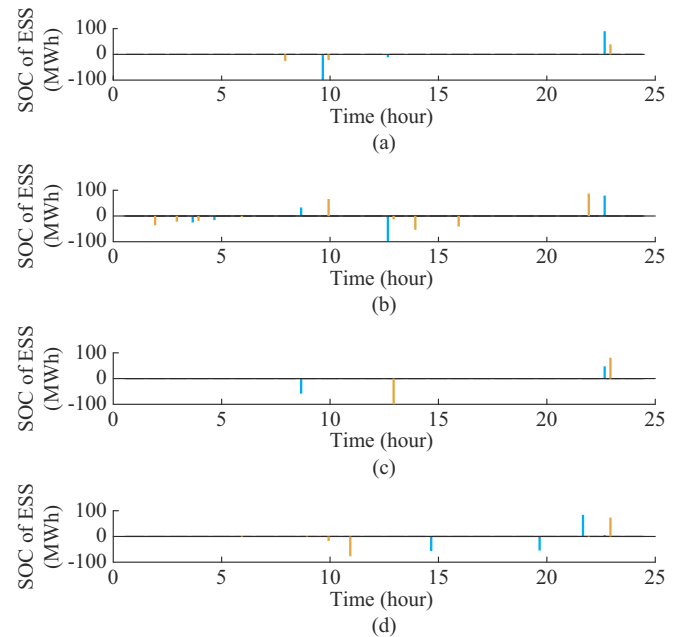


Fig. 9. Optimal charging and discharging statuses of energy storage system in 6-bus network. (a) Case 1. (b) Case 2. (c) Case 3. (d) Case 4.

Table III shows the effect of the number of outage lines on the objective function of the problem of unit commitment and the corresponding solution time in 6-bus network. It can be observed that with the increase in the number of outage lines, the objective function value of the problem and the solution time also increase. Besides, the demand response management program also has a high impact on the reduction of the objective function value. For example, when 4 lines are disconnected from the network, if 0% load shifting is considered, the objective function value is equal to \$544464, while if 10% load shifting is considered, the objective function value decreases to \$534143, which shows the effect of flexible loads.

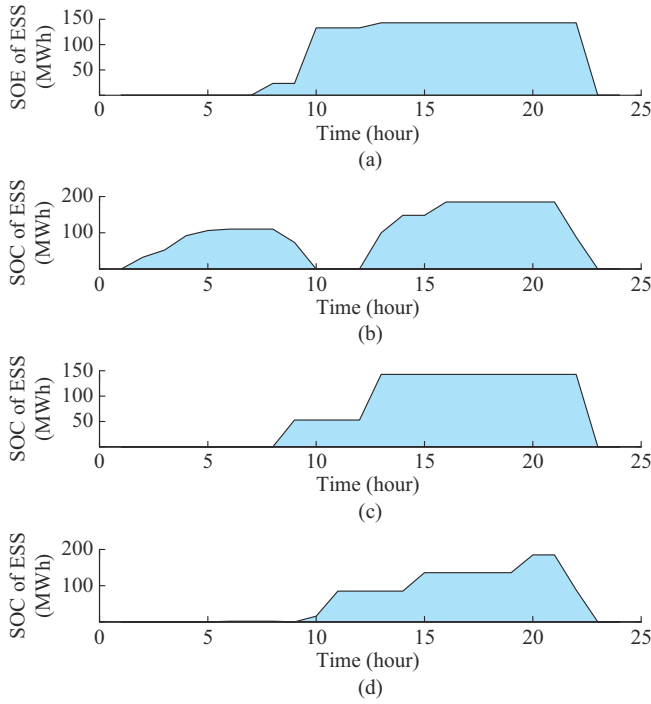


Fig. 10. Status of energy remaining in energy storage system in 6-bus network. (a) Case 1. (b) Case 2. (c) Case 3. (d) Case 4.

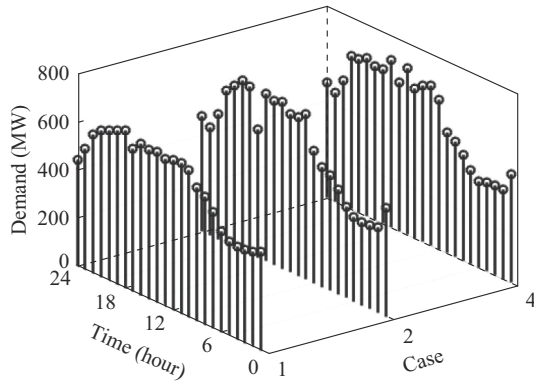


Fig. 11. Comparison of load shifting in different cases in 6-bus network.

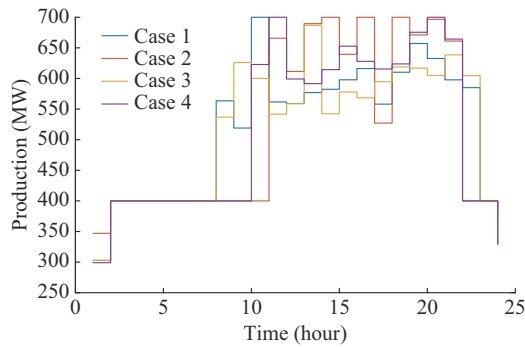


Fig. 12. Comparison of production of units in different cases in day-ahead operation in 6-bus network.

Table IV shows the effect of load shifting on the objective function of the unit commitment problem in the 6-bus network. It can be observed that with the increase of load shifting, the objective function value decreases significantly from \$535887 to \$524341.

TABLE III
EFFECT OF NUMBER OF OUTAGE LINES ON OBJECTIVE FUNCTION OF UNIT COMMITMENT PROBLEM AND CORRESPONDING SOLUTION TIME IN 6-BUS NETWORK

Load shifting (%)	Number of outage lines	No. of disconnected line	Objective function value (\$)	Solution time (s)
0	0		535756	5
	1	9	535887	6
	2	4, 9	535889	16
	3	2, 8, 9	535890	22
10	4	1, 4, 8, 9	544464	57
	0		529537	5
	1	9	529545	6
	2	2, 9	529638	8
	3	4, 8, 9	529738	19
	4	1, 4, 8, 9	534143	40

TABLE IV
EFFECT OF LOAD SHIFTING ON OBJECTIVE FUNCTION OF UNIT COMMITMENT PROBLEM IN 6-BUS NETWORK

Load shifting (%)	Objective function value (\$)	Load shifting (%)	Objective function value (\$)
0	535887	15	526232
5	532671	20	525171
10	529545	30	524341

B. 24-bus Network

In this subsection, the results related to the IEEE RTS 24-bus network shown in Fig. 13 are presented.

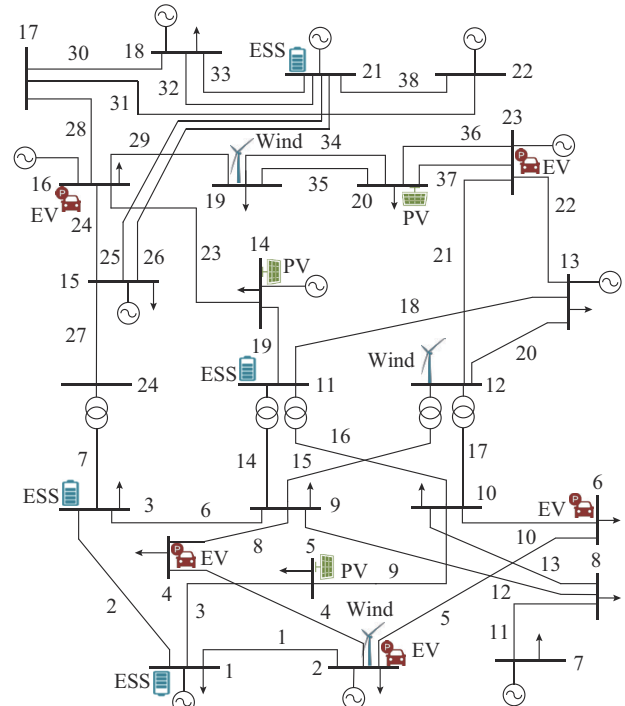


Fig. 13. Schematic of IEEE RTS 24-bus network.

To better analyze the proposed formulation, four different

case studies have been considered as follows.

Case 5: considering a maximum of 0% load shifting and the number of outage lines is equal to 1.

Case 6: considering a maximum of 10% load shifting and the number of outage lines is equal to 1.

Case 7: considering a maximum of 0% load shifting and the number of outage lines is equal to 5.

Case 8: considering a maximum of 10% load shifting and the number of outage lines is equal to 5.

The simulation results related to different cases in the 24-bus network are presented in Table V.

TABLE V
SIMULATION RESULTS OF DIFFERENT CASES IN 24-BUS NETWORK

Case	Objective function value (\$)	No. of outage lines
Case 5	2727219	8
Case 6	2719348	34
Case 7	2727226	1, 2, 7, 8, 12
Case 8	2719383	1, 6, 9, 12, 21

Table VI demonstrates the effect of load shifting on the objective function of the unit commitment problem in the 24-bus network. It can be observed that with the increase of the load shifting, the objective function value decreases significantly from \$272721 to \$271534.

TABLE VI
EFFECT OF LOAD SHIFTING ON OBJECTIVE FUNCTION OF UNIT COMMITMENT IN 24-BUS NETWORK

Load shifting (%)	Objective function value (\$)	Load shifting (%)	Objective function value (\$)
0	2727210	15	2717550
5	2721800	20	2716250
10	2719340	30	2715340

Figures 14-17 show the status of unit commitment of cases 5-8 in the 24-bus network for the day-ahead operation (1-24 hours), which indicate the modeling and accuracy of the unit commitment problem in each case. The numbers 1 and 0 indicate that the unit is on and off, respectively. It can be observed that with the change of load shifting and the number of outage lines, the status of unit commitment changes. As can be observed from Figs. 14-17, the status of Units 6 and 5 is the main difference between each case.

Figure 18 shows the optimal charging and discharging statuses of EV parking in different cases. The negative vertical axis indicates charging of EVs, while the positive vertical axis indicates discharging of EVs. The optimal charging and discharging statuses of EV parking located in buses 2, 4, 6, 16, and 23 are shown in green, orange, blue, purple, and pink colors, respectively. It can be observed that the charging and discharging statuses of EV parking are different in each case. Similarly, Fig. 19 shows the energy status of EV parking in cases 5-8 in the 24-bus network. Figures 18 and 19 prove the high accuracy of the proposed formulation in any number of EV parking under any condition.

Unit	1	2	3	4	5	6	7	8	9	10	11	12	13	14	15	16	17	18	19	20	21	22	23	24
Unit 10	1	1	1	1	1	1	1	1	1	1	1	1	1	1	1	1	1	1	1	1	1	1	1	1
Unit 9	0	0	0	0	0	0	0	1	1	1	1	1	1	1	1	1	1	1	1	1	1	1	1	0
Unit 8	0	0	0	0	0	0	0	0	0	0	0	0	0	0	0	0	0	0	0	0	0	0	0	0
Unit 7	0	0	0	0	0	0	0	0	0	0	0	0	0	0	0	0	0	0	0	0	0	0	0	0
Unit 6	0	0	0	0	0	0	1	1	1	1	1	1	1	1	1	1	1	1	1	1	1	1	1	0
Unit 5	0	0	0	0	0	0	0	0	0	1	1	1	1	1	1	1	1	1	1	1	1	1	1	1
Unit 4	1	1	1	1	1	1	1	1	1	1	1	1	1	1	1	1	1	1	1	1	1	1	1	1
Unit 3	1	1	1	1	1	1	1	1	1	1	1	1	1	1	1	1	1	1	1	1	1	1	1	1
Unit 2	1	1	1	1	1	1	1	1	1	1	1	1	1	1	1	1	1	1	1	1	1	1	1	1
Unit 1	1	1	1	1	1	1	1	1	1	1	1	1	1	1	1	1	1	1	1	1	1	1	1	1

Fig. 14. Status of unit commitment in 24-bus network in case 5.

Unit	1	2	3	4	5	6	7	8	9	10	11	12	13	14	15	16	17	18	19	20	21	22	23	24
Unit 10	1	1	1	1	1	1	1	1	1	1	1	1	1	1	1	1	1	1	1	1	1	1	1	1
Unit 9	0	0	0	0	0	0	1	1	1	1	1	1	1	1	1	1	1	1	1	1	1	1	1	0
Unit 8	0	0	0	0	0	0	0	0	0	0	0	0	0	0	0	0	0	0	0	0	0	0	0	0
Unit 7	0	0	0	0	0	0	0	0	0	0	0	0	0	0	0	0	0	0	0	0	0	0	0	0
Unit 6	0	0	0	1	1	1	1	1	1	1	1	1	1	1	1	1	1	1	1	1	1	1	1	1
Unit 5	0	0	0	0	0	0	0	0	0	0	0	0	0	0	0	1	1	1	1	1	1	1	1	1
Unit 4	1	1	1	1	1	1	1	1	1	1	1	1	1	1	1	1	1	1	1	1	1	1	1	1
Unit 3	1	1	1	1	1	1	1	1	1	1	1	1	1	1	1	1	1	1	1	1	1	1	1	1
Unit 2	1	1	1	1	1	1	1	1	1	1	1	1	1	1	1	1	1	1	1	1	1	1	1	1
Unit 1	1	1	1	1	1	1	1	1	1	1	1	1	1	1	1	1	1	1	1	1	1	1	1	1

Fig. 15. Status of unit commitment in 24-bus network in case 6.

Unit	1	2	3	4	5	6	7	8	9	10	11	12	13	14	15	16	17	18	19	20	21	22	23	24
Unit 10	1	1	1	1	1	1	1	1	1	1	1	1	1	1	1	1	1	1	1	1	1	1	1	1
Unit 9	0	0	0	0	0	0	0	1	1	1	1	1	1	1	1	1	1	1	1	1	1	1	1	0
Unit 8	0	0	0	0	0	0	0	0	0	0	0	0	0	0	0	0	0	0	0	0	0	0	0	0
Unit 7	0	0	0	0	0	0	0	0	0	0	0	0	0	0	0	0	0	0	0	0	0	0	0	0
Unit 6	0	0	0	0	0	0	1	1	1	1	1	1	1	1	1	1	1	1	1	1	1	1	1	0
Unit 5	0	0	0	0	0	0	0	0	0	0	1	1	1	1	1	1	1	1	1	1	1	1	1	1
Unit 4	1	1	1	1	1	1	1	1	1	1	1	1	1	1	1	1	1	1	1	1	1	1	1	1
Unit 3	1	1	1	1	1	1	1	1	1	1	1	1	1	1	1	1	1	1	1	1	1	1	1	1
Unit 2	1	1	1	1	1	1	1	1	1	1	1	1	1	1	1	1	1	1	1	1	1	1	1	1
Unit 1	1	1	1	1	1	1	1	1	1	1	1	1	1	1	1	1	1	1	1	1	1	1	1	1

Fig. 16. Status of unit commitment in 24-bus network in case 7.

Unit	1	2	3	4	5	6	7	8	9	10	11	12	13	14	15	16	17	18	19	20	21	22	23	24
Unit 10	1	1	1	1	1	1	1	1	1	1	1	1	1	1	1	1	1	1	1	1	1	1	1	1
Unit 9	0	0	0	0	0	0	1	1	1	1	1	1	1	1	1	1	1	1	1	1	1	1	1	0
Unit 8	0	0	0	0	0	0	0	0	0	0	0	0	0	0	0	0	0	0	0	0	0	0	0	0
Unit 7	0	0	0	0	0	0	0	0	0	0	0	0	0	0	0	0	0	0	0	0	0	0	0	0
Unit 6	0	0	0	1	1	1	1	1	1	1	1	1	1	1	1	1	1	1	1	1	1	1	1	1
Unit 5	0	0	0	0	0	0	0	0	0	0	0	0	0	0	0	1	1	1	1	1	1	1	1	1
Unit 4	1	1	1	1	1	1	1	1	1	1	1	1	1	1	1	1	1	1	1	1	1	1	1	1
Unit 3	1	1	1	1	1	1	1	1	1	1	1	1	1	1	1	1	1	1	1	1	1	1	1	1
Unit 2	1	1	1	1	1	1	1	1	1	1	1	1	1	1	1	1	1	1	1	1	1	1	1	1
Unit 1	1	1	1	1	1	1	1	1	1	1	1	1	1	1	1	1	1	1	1	1	1	1	1	1

Fig. 17. Status of unit commitment in 24-bus network in case 8.

Figure 20 shows a comparison of load shifting in different cases in the 24-bus network. It can be observed that the load shifting is different in each case. By comparing cases 5 and 6, we can observe that by the demand-side management, the peak load decreases from 2850 MW to 2650 MW.

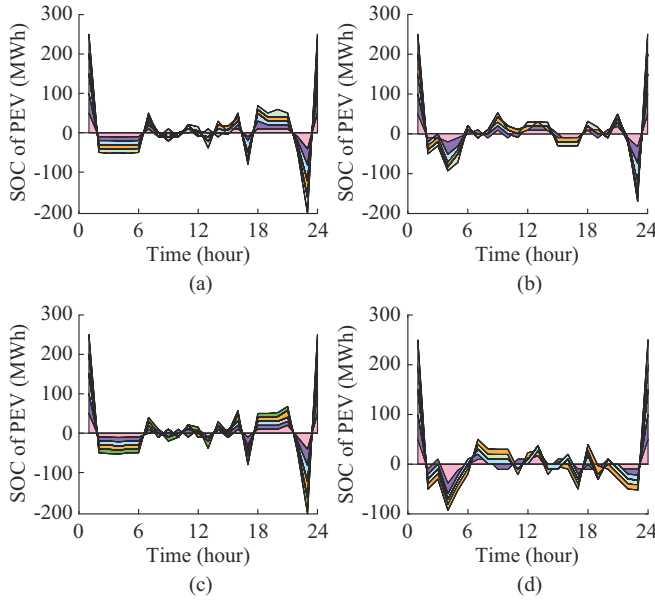


Fig. 18. Comparison of charging and discharging statuses of EVs in 24-bus network. (a) Case 5. (b) Case 6. (c) Case 7. (d) Case 8.

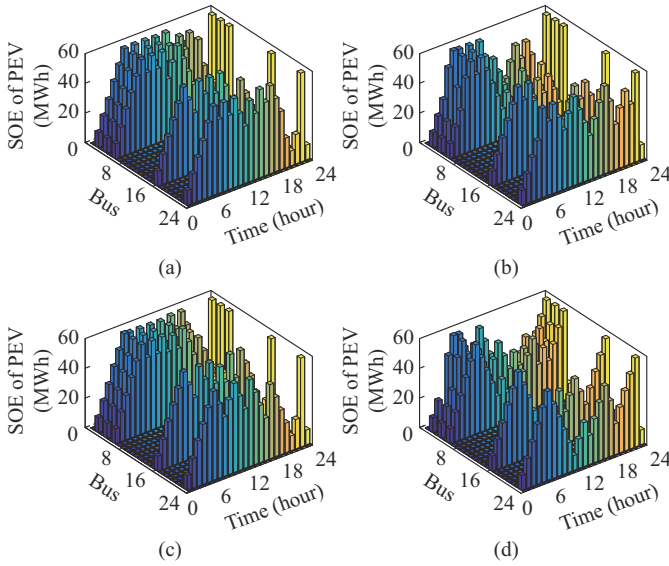


Fig. 19. Comparison of energy status of EV parking in cases 5-8 in 24-bus network. (a) Case 5. (b) Case 6. (c) Case 7. (d) Case 8.

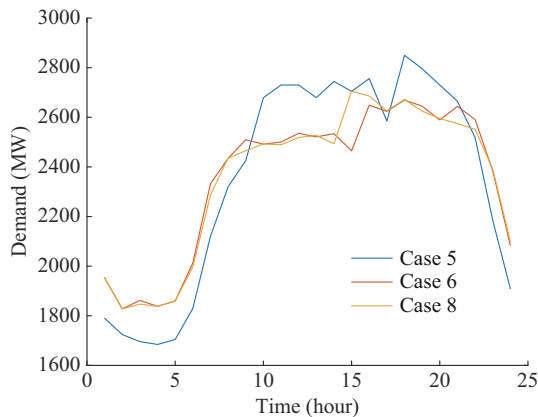


Fig. 20. Comparison of load shifting in different cases in 24-bus network.

Besides, with the increase of the number of outage lines, the peak load increases in case 8 compared with case 6. Figure 21 shows the production of units in different cases in the day-ahead operation in the 24-bus network. It can be observed that the demand-side management as well as the number of outage lines affects the production of units.

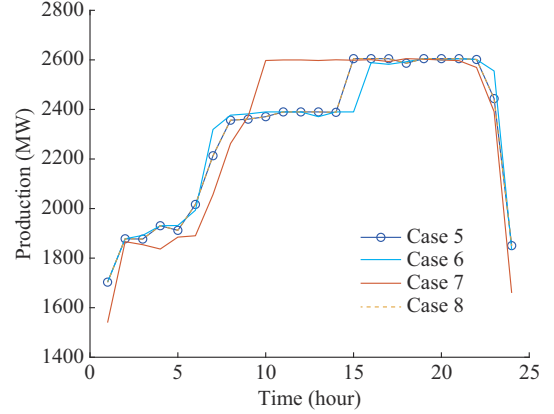


Fig. 21. Comparison of production of units in different cases in day-ahead in 24-bus network.

By examining the results obtained from the 6- and 24-bus networks, it can be found that the proposed formulation, in addition to being efficient, can be easily implemented and implemented for any system with any dimension.

IV. CONCLUSION

In this study, a formulation for modeling the problem of stochastic security-constrained unit commitment is presented. The proposed formulation is considered as an MILP model, which includes modeling of charging and discharging of large-scale EVs, optimal charging and discharging of energy storage systems, and demand-side management along with renewable energy resources. A multi-objective function is considered to minimize different objectives in order to get the maximum efficiency from the proposed formulation. The 6-bus and 24-bus networks are considered for analysis with different cases. The results demonstrate that by managing the demand and optimal charging and discharging of batteries and EVs in the unit commitment problem, it is possible to reduce the effect of line outages on the performance of the objective function. For example, the objective function value only differs by 0.015% for the cases with 1 outage line and 5 outage lines. Besides, the proposed formulation can be well implemented in different transmission networks. Also, various cases considered by changing the parameters of the problem to investigate the demand-side management performance in the problem of unit commitment show that the proposed formulation has good scalability. However, as we know, by modeling very large transmission networks, the numbers of variables and parameters of the proposed problem increase dramatically. Therefore, one of the leading limitations of this work is to solve it by solvers.

To continue this paper, the following items are suggested for future research.

1) Modeling distribution networks in each bus of the trans-

mission network, so as to analyze the proposed formulation of the transmission network in distribution networks.

2) Modeling the natural gas network along with the transmission network, so as to analyze the impact of natural gas reduction on gas-fired power plants in the power grid.

3) Presenting a bi-level optimization model with the aim of maximizing the resilience of the transmission network to the proposed formulation in times of natural disasters.

4) Adding the discussion of network resilience to the proposed formulation and modeling natural disasters and cyber-attacks on the network.

APPENDIX A

Power levels of renewable energy resources for each scenario can be expressed as:

$$g_{b,t,s}^r = g_{b,t,s}^{r,f} + \Delta g_{b,t,s}^r \quad \forall b \in B, t \in T, s \in S \quad (A1)$$

where $g_{b,t,s}^{r,f}$ is the forecast value of renewable power; and $\Delta g_{b,t,s}^r$ is the forecast error of the renewable power. Since each scenario has a probability of occurrence, the normalized probability of each generated scenario is obtained using the following equation.

$$\pi_s = \frac{\prod_{t=1}^T \prod_{b=1}^B \left(\sum_{r=1}^R \varrho_{r,b,t,s}^r \beta_{r,t} \right)}{\sum_{s=1}^S \prod_{t=1}^T \prod_{b=1}^B \left(\sum_{r=1}^R \varrho_{r,b,t,s}^r \beta_{r,t} \right)} \quad (A2)$$

where $\beta_{r,t}$ is the probability of the r^{th} renewable power interval at time t ; and $\varrho_{r,b,t,s}^r$ is a binary parameter indicating whether the r^{th} renewable power interval of renewable energy resource on bus b is selected in scenario s ($\varrho_{r,b,t,s}^r = 1$) or not ($\varrho_{r,b,t,s}^r = 0$) at time t . The full description of the scenario generation method can be found in [22].

REFERENCES

- [1] H. Zhou, K. Yuan, and C. Lei, "Security constrained unit commitment based on modified line outage distribution factors," *IEEE Access*, vol. 10, pp. 25258-25266, Mar. 2022.
- [2] Y. Yin, C. He, T. Liu *et al.*, "Risk-averse stochastic midterm scheduling of thermal-hydro-wind system: a network-constrained clustered unit commitment approach," *IEEE Transactions on Sustainable Energy*, vol. 13, no. 3, pp. 1293-1304, Jul. 2022.
- [3] M. Said, E. H. Houssein, S. Deb *et al.*, "A novel gradient based optimizer for solving unit commitment problem," *IEEE Access*, vol. 10, pp. 18081-18092, Feb. 2022.
- [4] Z. Jiang, Y. Liu, Z. Kang *et al.*, "Security-constrained unit commitment for hybrid VSC-MTDC/AC power systems with high penetration of wind generation," *IEEE Access*, vol. 10, pp. 14029-14037, Jan. 2022.
- [5] Q. Gao, Z. Yang, W. Yin *et al.*, "Internally induced branch-and-cut acceleration for unit commitment based on improvement of upper bound," *IEEE Transactions on Power Systems*, vol. 37, no. 3, pp. 2455-2458, May 2022.
- [6] X. Chen, Y. Yang, Y. Liu *et al.*, "Feature-driven economic improvement for network-constrained unit commitment: a closed-loop predict-and-optimize framework," *IEEE Transactions on Power Systems*, vol. 37, no. 4, pp. 3104-3118, Jul. 2022.
- [7] G. E. Constante-Flores, A. J. Conejo, and F. Qiu, "AC network-constrained unit commitment via relaxation and decomposition," *IEEE Transactions on Power Systems*, vol. 37, no. 3, pp. 2187-2196, May 2022.
- [8] G. Gutiérrez-Alcaraz, B. Díaz-López, J. M. Arroyo *et al.*, "Large-scale preventive security-constrained unit commitment considering $N-k$ line outages and transmission losses," *IEEE Transactions on Power Systems*, vol. 37, no. 3, pp. 2032-2041, May 2022.
- [9] Y. Zhang H. Cui, J. Liu *et al.*, "Encoding frequency constraints in preventive unit commitment using deep learning with region-of-interest active sampling," *IEEE Transactions on Power Systems*, vol. 37, no. 3, pp. 1942-1955, May 2022.
- [10] T. Wu, Y.-J. A. Zhang, and S. Wang, "Deep learning to optimize: security-constrained unit commitment with uncertain wind power generation and BESSs," *IEEE Transactions on Sustainable Energy*, vol. 13, no. 1, pp. 231-240, Jan. 2022.
- [11] K. Doubleday, J. D. Lara, and B.-M. Hodge, "Investigation of stochastic unit commitment to enable advanced flexibility measures for high shares of solar PV," *Applied Energy*, vol. 321, p. 119337, Sept. 2022.
- [12] O. Egbue, C. Uko, A. Aldubaisi *et al.*, "A unit commitment model for optimal vehicle-to-grid operation in a power system," *International Journal of Electrical Power & Energy Systems*, vol. 141, p. 108094, Oct. 2022.
- [13] X. Cheng, S. Feng, H. Zheng *et al.*, "A hierarchical model in short-term hydro scheduling with unit commitment and head-dependency," *Energy*, vol. 251, p. 123908, Jul. 2022.
- [14] Y. Sun, B. Wang, R. Yuan *et al.*, "Rolling unit commitment based on dual-discriminator conditional generative adversarial networks," *Electric Power Systems Research*, vol. 205, p. 107770, Apr. 2022.
- [15] H. Q. Truong and C. Jeenanunta, "Fuzzy mixed integer linear programming model for national level monthly unit commitment under price-based uncertainty: a case study in Thailand," *Electric Power Systems Research*, vol. 209, p. 107963, Aug. 2022.
- [16] P. Mansourshoar, A. S. Yazdankhah, M. Vatanpour *et al.*, "Impact of implementing a price-based demand response program on the system reliability in security-constrained unit commitment problem coupled with wind farms in the presence of contingencies," *Energy*, vol. 255, p. 124333, Sept. 2022.
- [17] J. Xu, Y. Ma, K. Li *et al.*, "Unit commitment of power system with large-scale wind power considering multi time scale flexibility contribution of demand response," *Energy Reports*, vol. 7, pp. 342-352, Nov. 2021.
- [18] G. E. Constante-Flores, A. J. Conejo, and F. Qiu, "AC network-constrained unit commitment via conic relaxation and convex programming," *International Journal of Electrical Power & Energy Systems*, vol. 134, p. 107364, Jan. 2022.
- [19] C. Zhang and L. Yang, "Distributed AC security-constrained unit commitment for multi-area interconnected power systems," *Electric Power Systems Research*, vol. 211, p. 108197, Oct. 2022.
- [20] P. Liang and N. Bohloli, "Optimal unit commitment integrated energy storage system, renewable energy sources and FACTS devices with robust method," *Electric Power Systems Research*, vol. 209, p. 107961, Aug. 2022.
- [21] H. Karimianfard, H. Haghighat, and B. Zeng, "Co-optimization of battery storage investment and grid expansion in integrated energy systems," *IEEE Systems Journal*, vol. 16, no. 4, pp. 5928-5938, Dec. 2022.
- [22] B. Bahmani-Firouzi, E. Farjah, and R. Azizpanah-Abarghoee, "An efficient scenario-based and fuzzy self-adaptive learning particle swarm optimization approach for dynamic economic emission dispatch considering load and wind power uncertainties," *Energy*, vol. 50, pp. 232-244, Feb. 2013.

Ali Gholami Trojani received the master's degree from Islamic Azad University Damghan Branch, Damghan, Iran, in 2015. Currently, he is pursuing the Ph. D. degree in electrical engineering at Islamic Azad University Damghan Branch. His research interests include distribution and transmission optimization.

Mahmoud Samiei Moghaddam received the master's degree from Khaje Nasir University, Tehran, Iran, in 2005, and the Ph.D. degree in electrical engineering from K. N. Toosi University of Technology, Tehran, Iran, in 2016. Since 2005, he has been a Faculty Member of Islamic Azad University Damghan Branch, Damghan, Iran. His research interests include power system planning and electric vehicles.

Javad Mohamadi Baigi received the Ph.D. degree in aerospace engineering from Amirkabir University of Technology, Tehran, Iran, in 2008. Since 2005, he has been a Faculty Member of Islamic Azad University Damghan Branch, Damghan, Iran. His research interests include smart grids and energy storage system.